1  Removal of the waterborne protozoan parasites *Cryptosporidium* and *Giardia* by

2  photochemical processes, ultrasound and adsorption onto granular activated carbon

3

4

5  M.J. Abeledo-Lameiro[a], S. Couso-Pérez[b,c], E. Ares-Mazás[b], H. Gómez-Couso[b,d*].

6

7  [a] Plataforma Solar de Almería–CIEMAT, Carretera Senés, Km 4.5, 04200, Tabernas, Almería,

8  Spain, [b] Laboratory of Parasitology, Department of Microbiology and Parasitology, Faculty of

9  Pharmacy, University of Santiago de Compostela, 15782 Santiago de Compostela, A Coruña,

10  Spain, [c] Nanotechnology and Integrated BioEngineering Centre, School of Engineering, Ulster

11  University, Newtownabbey BT37 0QB, United Kingdom, [d] Research Institute on Chemical and

12  Biological Analysis, University of Santiago de Compostela, 15782 Santiago de Compostela, A

13  Coruña, Spain

14

15

16

17

18

19

20  *corresponding email address: hipolito.gomez@usc.es

21 ABSTRACT

22 *Cryptosporidium* and *Giardia* are two important genera of intestinal protozoan

23 parasites that infect a wide range of vertebrate hosts, including humans. The route of

24 transmission for these enteropathogens is the faecal-oral route, directly from person

25 to person or animal to person, or indirectly via contaminated food and water, being the

26 latter the most common route. They cause the self-limited illnesses cryptosporidiosis

27 and giardiosis, which symptoms depend on the immunity status of the host, varying

28 from asymptomatic to diarrhoea, malaise or fatigue, abdominal pain, anorexia and

29 weight loss. The infective forms, oocysts and cysts (oo/cysts), are highly resistant to

30 environmental conditions and to the conventional disinfection treatments of water.

31 Thus, oo/cysts have been reported to occur in different types of water (surface water,

32 drinking water, wastewater) being identified in waterborne outbreaks worldwide.

33 Therefore, new technologies that enhance or optimize conventional methods are

34 needed. This chapter reviews the current knowledge about the efficacy of different

35 technologies that can be applied in the removal of *Cryptosporidium* and *Giardia* from

36 water such as photochemical advanced oxidation processes (AOPs), ultrasound (a

37 non-photochemical AOPs) and granular activated carbon adsorption.

## 9.1 *Cryptosporidium* and *Giardia*

*Cryptosporidium* and *Giardia* are genera of important protozoan parasites that infect the gastrointestinal epithelium of a wide range of vertebrate hosts, including humans. They cause the self-limited illnesses cryptosporidiosis and giardiosis, which symptoms depend on the immunity status of the host, varying from asymptomatic to diarrhoea, malaise or fatigue, abdominal pain, anorexia and weight loss. Human cryptosporidiosis and giardiosis have a worldwide distribution, which prevalence vary depending upon the geographical area and the level of environmental health. Thus, in developing countries, prevalences between 0 and 13.7% for cryptosporidiosis and from 8.0 to 30.0% for giardiosis have been reported, although values up to 69.6% and 33.0% have been found, respectively. In developed countries, prevalences from 0.3 to 54.2% for *Cryptosporidium* and from 1.0 to 8.0% for *Giardia* have been observed, probably because of the existence of surveillance systems for routine detection of *Cryptosporidium* and *Giardia*[1-3]. In addition, most outbreaks of infection associated with recreational or drinking water have been reported in these countries[4-6]. In this respect, during the period from 2017 to 2020, 86.1% of the waterborne parasitic protozoan outbreaks occurred in the United States (56.2%), United Kingdom (20.3%) and New Zealand (9.6), with *Cryptosporidium* spp. and *Giardia duodenalis* (syn. *Giardia lamblia*, *Giardia intestinalis*) being the most common aetiological agents, as they were reported in 95.6% (240/251) of outbreaks[7].

*Cryptosporidium* is a genus of the family Cryptosporidiidae, order Eucoccidiarida, subclass Cryptogregaria, class Sporozoasida, and phylum Apicomplexa that present at least 44 species and more than 120 genotypes, among them 19 species and 4 genotypes have been reported in humans, being *Cryptosporidium parvum* (zoonotic) and *Cryptosporidium hominis* (anthroponotic), the most prevalent species[8]. The oocyst

is the resistance form of *Cryptosporidium* (size of 3-8 µm in diameter) and the responsible of its transmission. Each oocyst contains four infective sporozoites enclosed by a trilaminar wall extremely resistant that allow it to survive for months in moist ambient conditions and resists the disinfectant more commonly used in water disinfection, enabling foodborne and waterborne transmission[9-11].

*Cryptosporidium* has a complex and monoxenous life cycle that completes in a single host (sexual and asexual reproduction sequentially in the same host)[12,13] (Figure 9.1). Infection is initiated by the ingestion of sporulated oocysts. The sporozoites are released through a suture in the oocyst wall due to the response to body temperature, gastric acids, trypsin and biliary salts, and then attach to the apical surface of epithelial cells where they are internalized within the cell plasmalemma by an active invasion mechanism until they become enclosed within a parasitophorous vacuole (PV) with intracellular but extracytoplasmic location. Inside the PV, the parasite develops into spherical trophozoites, which undergo asexual replication (merogony) to produce type I meronts containing 6-8 merozoites. When the PV breaks, type I merozoites are released and can infect adjacent cells, where they undergo asexual multiplication to produce additional type I meronts, or type II meronts, which contain 4 type II merozoites. Upon infecting new host cells, type II merozoites differentiate to microgamonts or macrogamonts[14,15]. Each microgamont becomes multinucleate and each nucleus is incorporated into a microgamete. Microgametes are released and fertilize the quiescent macrogamete. Fertilization produces a zygote, which undergoes meiosis to produce 4 sporozoites. The sporulated oocysts are released to the intestinal lumen as thin-walled oocysts of double-layered membrane or thick-walled oocysts with three-layered membrane[13]. The thin-walled oocysts (approximately 20%) excyst inside the same host and enable maintenance of the infection, obviating the need for a new

88  oral infection and whereby acute diarrhoea is prolonged and large quantities of oocysts

89  are released by infected hosts[16]. However, 80% of the thick-walled oocysts are

90  released with the faeces and, as these are environmentally resistant forms, they are

91  responsible for the transmission of infection from one host to other susceptible hosts

92  (Figure 9.1).

93                              [Insert Figure 9.1 here]

94  *Giardia* is a genus of flagellated protozoans that belongs to the order Diplomonadida,

95  class Zoomastigophora and the phylum Sarcomastigophora. Currently, there are 9

96  validated *Giardia* spp. in several vertebrate hosts and 8 genotypes of *G. duodenalis* in

97  mammals, named as assemblages A to H, being the species *G. duodenalis* and the

98  assemblages A and B the only reported in humans[8]. *Giardia* species have two major

99  stages in the life cycle, the trophozoite and the cyst. The trophozoite inhabits and

100 multiplied in the upper small intestine of infected hosts, causing the clinical

101 manifestations. The cyst is very resistant and is eliminated by the faeces, being

102 responsible for the transmission[17].

103 Morphologically, the trophozoite of *G. duodenalis* has a piriform shape, bilateral

104 symmetry, and presents a length of 12-15 µm and a width of 5-9 µm. Besides, it has

105 eight flagella: two anterior, two posterior, two caudal and two ventral. On the ventral

106 side, the trophozoite has a structure in form of a lobulated disk which is the part where

107 the parasite is fixed on the surface of the intestine. On the dorsal side are two oval

108 nuclei with large endosomes[18]. The cyst has an oval form with a size of 8-12 µm of

109 length and 6-10 µm of width and presents a transparent wall of 0.3-0.5 µm of thickness.

110 In the phase of maturation, inside of the cyst appear four nuclei placed at one of the

111 poles[18].

112    Infection of a susceptible host become when the cyst is ingested with contaminated

113    water or food or through direct contact with an infected host. After the ingestion of the

114    cyst, the exposure to the acid environment of the stomach and later to the biliary salts

115    in the duodenum, the cyst releases two trophozoites in the lumen of the proximal small

116    intestine. The trophozoites are the vegetative form and adhere through the ventral disk

117    at the surface of intestinal microvilli below the mucoid and become multiplied by

118    longitudinal binary fission. Then, they reach the lower part of the small intestine

119    through the intestinal matter, and there they begin to transform into oval cysts in

120    response to the reduction of cholesterol and the digestion of lipids. Hereafter, the cysts

121    pass by the large intestine, finally being released to the outside with the faeces of the

122    host[17,19](Figure 9.2).

123                                [Insert Figure 9.2 here]

124    Waterborne cryptosporidiosis and giardiosis are globally emerging public health

125    issues[7]. Several studies have demonstrated the presence of *Cryptosporidium* oocysts

126    and *Giardia* cysts in different types of water (surface waters, drinking water,

127    recreational waters and wastewater treatment plant effluents)[20]. Water bodies may be

128    directly contaminated with faecal residues from humans or animals or indirectly by run-

129    off from contaminated surfaces[21-23]. Moreover, water systems may also be

130    contaminated by sewage or effluents from wastewater treatment plants, which

131    treatments are insufficient to totally remove the infective forms of *Cryptosporidium* and

132    *Giardia*[24-26]. In this way and taking into account that the average overall human

133    excretion rate is estimated to be $10^6$ to $10^8$ oo/cysts per person/year, the estimated

134    total global human emissions are $10^{17}$ oo/cysts per year, with the urban population

135    being responsible for the 89.0% of emissions[27,28]. Thus, the concentration of oocysts

136    of *Cryptosporidium* in river water was predicted using a mathematical model

developed by Vermeulen, et al. [26], which established values of between $10^{-6}$ and $10^2$ oocysts/L worldwide. Furthermore, Hofstra and Vermeulen [28] predicted an increase of up to 70% in human *Cryptosporidium* emissions, with higher concentrations of this waterborne protozoan in surface waters due to population growth in developing countries. In the case of *Giardia*, the estimated concentration of cysts in surface waters worldwide ranges from $10^{-3}$ and $10^2$ cysts/L[20].

The existence of waterborne outbreaks caused by these enteroprotozoan parasites reveals that oo/cysts cannot be eliminated totally by conventional disinfection water treatments based on physical, chemical and biological methods. Therefore, new technologies are needed to improve water treatments and to prevent the contamination of the environment and, consequently water supplies and water sources, by these waterborne protozoan parasites. Advanced oxidation processes (AOPs) are a group of related technologies that lead to the generation of reactive oxygen species (ROS), mainly the hydroxyl radical (HO$^\bullet$), which results in the oxidative degradation of pollutants and inactivation of several waterborne pathogens. This chapter reviews the current knowledge about the efficacy of photochemical AOPs in the removal of *Cryptosporidium* and *Giardia* from water, as well as ultrasound, a non-photochemical AOPs, and granular activated carbon adsorption.

**9.2 Photochemical processes in the inactivation of protozoan parasites in water**

AOPs are oxidative processes that involve the formation of HO$^\bullet$, which has the second oxidizing potential after fluorine. These radicals are capable of non-selective oxidizing and mineralizing a wide variety of organic molecules, allowing the degradation of recalcitrant and emerging contaminants and the inactivation of different

160 microorganisms in water. AOPs investigated for application in water treatment include

161 photochemical and non-photochemical processes[29].

162 The term photocatalysis was first defined by Carey, et al. [30] in 1976 as the acceleration

163 of a photoreaction through the presence of a catalyst, with light and a catalyst being

164 essential. In this way, chemical species are altered as a result of the absorption of

165 ultraviolet (UV)-visible radiation by a photosensitive species, the catalyst.

166 Heterogeneous photocatalysis is based on the use of a solid semiconductor (e.g.

167 titanium dioxide, zinc oxide, zinc sulphide, cadmium sulphide and iron oxides)

168 irradiated with photons of the appropriate wavelength to generate a reaction at the

169 solid-liquid or solid-gas interface. By definition, the catalyst must be able to be reused

170 after acting in the oxidation-reduction system without undergoing significant

171 changes[31]. On the contrary, in homogeneous photocatalysis, all of the components

172 are at the same phase, generally dissolved in the liquid phase, and copper and iron
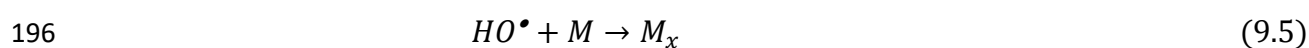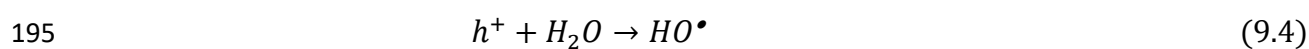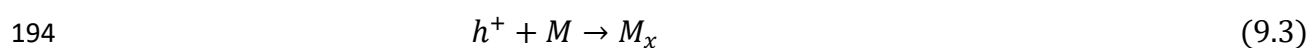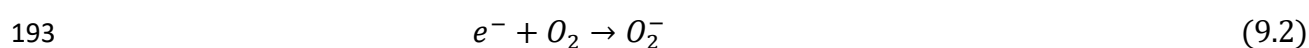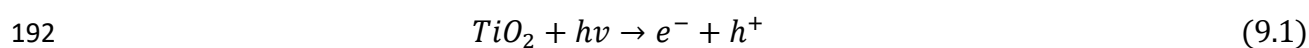
173 salts are often used[32].

**9.2.1. Heterogeneous photocatalysis with titanium dioxide ($TiO_2$)**

175 In the last few decades, the degradation of chemical compounds by photocatalytic or

176 photochemical processes has gained importance in the area of wastewater treatment,

177 although, water disinfection is also very important in photocatalytic processes. Among

178 the AOPs, heterogeneous photocatalysis with $TiO_2$ is the most widely investigated,

179 particularly as a tertiary treatment for the degradation of chemical pollutants present

180 in water[32,33].

181 Photocatalysis with $TiO_2$ can be carried out by maintaining the catalyst immobilized in

182 a solid support or in aqueous suspension. The choice of one method or the other will

183 depend on the final destination of the treated water. Thus, for purifying of drinking

184    water, $TiO_2$ must be immobilized, whereas in wastewater treatment, the photocatalyst

185    can be used in suspension, providing a larger surface area of contact. In addition to

186    latter reuse, it is possible to recover $TiO_2$ by different methods, some as simple as

187    sedimentation[34] and others based on the use of filters and/or coagulating agents[35,36].

188    In heterogeneous photocatalysis with $TiO_2$, organic compounds (M) are oxidized ($M_x$)

189    through the valence band opening while oxygen is reduced[37,38]. The positive opening

190    can also react with water, forming $HO^\bullet$ [32,39], which can further oxidize organic

191    compounds[37,40] (Figure 9.3):

192
$$TiO_2 + hv \rightarrow e^- + h^+ \tag{9.1}$$

193
$$e^- + O_2 \rightarrow O_2^- \tag{9.2}$$

194
$$h^+ + M \rightarrow M_x \tag{9.3}$$

195
$$h^+ + H_2O \rightarrow HO^\bullet \tag{9.4}$$

196
$$HO^\bullet + M \rightarrow M_x \tag{9.5}$$

197                    [Insert Figure 9.3 here]

198    Numerous studies have demonstrated that solar photocatalysis with $TiO_2$ is effective

199    for inactivating a wide range of microorganisms present in water, air and on surfaces:

200    algae, unicellular and filamentous fungi, Gram-negative and Gram-positive bacteria,

201    mammalian viruses and bacteriophages[41-47]. However, bacterial endospores, fungal

202    spores and protozoan oo/cysts are very resistant to $TiO_2$ photocatalytic process

203    because they have robust cell walls[32,33,38,39,48].

204    Studies involving $TiO_2$ photocatalytic processes and *Cryptosporidium* or *Giardia* as

205    target pathogens are scarce and most of them have used immobilized $TiO_2$ and UV

206    lamps[49-60].

In a study evaluating the photocatalytic inactivation of *C. parvum* oocysts in aqueous solution, Otaki, et al. [49] used TiO$_2$ immobilized onto the bottom of a glass beaker irradiated with UV-A or UV-C light and observed that oocyst inactivation was significantly faster under UV-C irradiated TiO$_2$, suggesting a synergistic disinfection mechanism. Curtis, et al. [50] observed a 26% reduction in the viability of *C. parvum* oocysts present in tap water after 60 min of exposure to an electric field enhanced photoreactor comprising a Ti/TiO$_2$ electrode irradiated with UV-A. Navalon, et al. [56] described the disinfection activity of a silica-supported TiO$_2$ ceramic photocatalyst in 150 L of water spiked with *C. parvum* oocysts and recirculated at 500 L/h through a photoreactor fitted with UV-C lamp, showing that photocatalytic inactivation was much more efficient than UV irradiation alone. Sunnotel, et al. [57] observed oocyst inactivations of 73.7-78.4% in buffer solution and river water after 3 h of exposure to UV-A radiation in presence of TiO$_2$ immobilized.

Under natural solar conditions, Méndez-Hermida, et al. [52] investigated photocatalytic disinfection by assessing the inactivation of *C. parvum* oocysts in 2 mL-bottle reactors filled with drinking water and containing TiO$_2$ immobilized onto plastic sheets. After 8 and 16 h of overcast and cloudy solar irradiance conditions, the photocatalytic process reduced oocyst viability in 61.6% and 88.1%, respectively. Fontán Sainz [58] tested the use of compound parabolic collectors (CPCs) and immobilized TiO$_2$ to enhance solar inactivation of *C. parvum* in drinking water at pilot scale conditions (7 L) and a flow rate of 20 L/min. After 8 h of exposure to natural solar radiation, similar reductions in the oocyst viability were observed in reactors with and without TiO$_2$ (approximately, 50%).

Regarding the use of TiO$_2$ suspensions, only four studies have evaluated the efficacy of TiO$_2$ slurry for inactivating *C. parvum* oocysts[53,54,59,60]. Ryu, et al. [54] demonstrated

232    a synergistic effect of UV-C and TiO$_2$ suspensions (1 mg/L) in a volume of 14 mL of

233    buffered water, resulting in oocyst inactivation of 2 log and 3 log, although the authors

234    did not specify the exposure time. In a study involving higher TiO$_2$ concentrations (100,

235    500 and 1000 mg/L) and volume (50 mL), Cho and Yoon [53] investigated the

236    inactivation of *C. parvum* oocysts in phosphate buffer solution conferred in a reactor

237    irradiated with UV-A and reported a concentration × contact time (CT) value required

238    to achieve a 2 log reductions in the *C. parvum* viability with the HO$^\bullet$ of $7.9 \times 10^{-5}$ mg

239    min/L.

240    Abeledo-Lameiro, et al. [59] evaluated the capability of heterogeneous photocatalysis

241    with TiO$_2$ slurry (63, 100 and 200 mg/L) to inactivate *C. parvum* oocysts under

242    simulated solar conditions in distilled water (DW). The highest reduction in the oocyst

243    viability (95.5%) was observed at concentration of 100 mg/L of TiO$_2$ photocatalyst after

244    5 h of exposure to simulated solar radiation. This represented an improvement relative

245    to the results obtained with samples exposed without photocatalyst and with 63 mg/L

246    of TiO$_2$ (reductions of 51.4% and 41.7%, respectively), optimal concentration

247    estimated basing on the reactor dimensions, so that suspended catalyst uses 99% of

248    the incident radiation (Figure 9.4)[34].

249    Moreover, the same authors evaluated the efficacy of solar photocatalysis with TiO$_2$

250    slurry to inactivate *C. parvum* oocysts in a simulated wastewater treatment plant

251    (WWTP) effluent. However, the decreases in the oocyst viability detected in simulated

252    WWTP effluent were significantly lower than the corresponding values observed in

253    DW, even in comparison with the samples exposed without photocatalyst (50.7%;

254    28.6%; 26.5%; and 17.8% for samples containing 0, 63, 100 and 200 mg/L of TiO$_2$ in

255    simulated WWTP effluent, respectively)[59].

[Insert Figure 9.4 here]

257    On the other hand, and with the aim of accelerating the solar water disinfection

258    process, heterogeneous photocatalysis with $TiO_2$ has been combined with the addition

259    of readily available, inexpensive and safe oxidant compounds, such as hydrogen

260    peroxide ($H_2O_2$). Thus, several authors have demonstrated that the $TiO_2$ photocatalytic

261    disinfection process is enhanced by the addition of $H_2O_2$, effectively killing several

262    bacterial species such as *Escherichia coli*, *Staphylococcus epidermidis* and

263    *Staphylococcus mutans*[32,61,62]. In this sense, Abeledo-Lameiro, et al. [60] evaluated the

264    photocatalytic inactivation of *C. parvum* oocysts in DW using $TiO_2$ slurry (100 mg/L) in

265    combination of $H_2O_2$ (50 mg/L) under simulated and natural solar conditions. However,

266    in both simulated and natural solar conditions, the results obtained in the water

267    samples containing $TiO_2$/$H_2O_2$ were not statistically significant different from the

268    corresponding values observed in samples exposed exclusively with $TiO_2$ (reductions

269    in the oocyst viability of 95.4±2.4% *vs* 95.8±4.3% and 97.5±2.0% *vs* 98.9±0.7%

270    determined in samples containing $TiO_2$ and $TiO_2$/$H_2O_2$, under simulated and natural

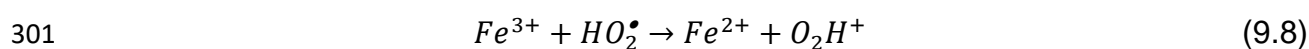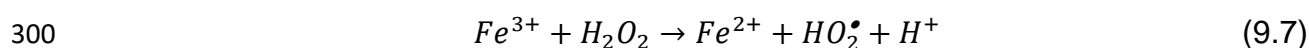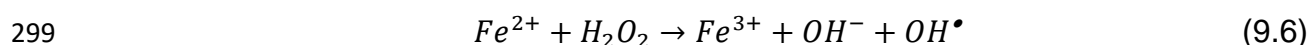271    solar radiations, respectively)[60].

272    Regarding *Giardia*, three studies have evaluated the inactivation of cysts by $TiO_2$

273    photocatalysis under UV-C and UV-A radiation[51,55,56]. Under UV-A lamps coated by

274    $TiO_2$, Lee, et al. [51] proved the inactivation of *G. duodenalis* cysts in DW after 2 h of

275    exposure. Navalon, et al. [56] evaluated the disinfection activity of a silica-supported

276    $TiO_2$ ceramic photocatalyst in 150 L of water recirculated at 500 L/h through a

277    photoreactor fitted with UV-C lamp, showing that 95.1% of the *G. duodenalis* cysts

278    were inactivated after 30 min of exposure. Finally, the inactivation of *G. duodenalis*

279    cysts was evaluated in the presence of 2 g/L of neat $TiO_2$ or silver loaded $TiO_2$,

280    demonstrating 6 log reductions in the cyst viability after 30 and 25 min of exposure to

281    the UV-C radiation, respectively[55].

282    The mechanism underlying photocatalytic inactivation is not yet clear. However,

283    numerous studies have investigated the generation of ROS and their interaction with

284    biological structures in an attempt to elucidate the inactivation mechanisms,

285    concluding that the leading cause of loss of microorganism viability is not yet

286    completely understood[33,63]. In this sense, several studies carried out with *C. parvum*

287    oocysts revealed the existence of morphological changes and the break of the suture

288    line in the oocyst wall after photocatalytic treatment, causing a spontaneous

289    excystation and the existence of empty oocysts[57,64]. Moreover, the damage in the

290    oocyst wall can cause an increase in its permeability and facilitate the penetration of

291    products with high oxidizing power derived from exposure to UV radiation[52].

292    **9.2.2. Homogeneous photocatalysis by photo-Fenton process**

293    Henry J. Fenton described the Fenton reaction in 1894, demonstrating that $H_2O_2$ could

294    be activated by $Fe^{2+}$ salts to oxidize tartaric acid in an aqueous solution[65]. In 1934,

295    $HO^\bullet$ was suggested to be the main compound responsible for the oxidative capacity

296    of the Fenton reaction[66]. The formation of $HO^\bullet$ in the homogeneous Fenton process in

297    absence of a light source is produced when $H_2O_2$ is decomposed by $Fe^{2+}$ ions

298    dissolved in the aqueous phase[67]:

299
$$Fe^{2+} + H_2O_2 \rightarrow Fe^{3+} + OH^- + OH^\bullet \tag{9.6}$$

300
$$Fe^{3+} + H_2O_2 \rightarrow Fe^{2+} + HO_2^\bullet + H^+ \tag{9.7}$$

301
$$Fe^{3+} + HO_2^\bullet \rightarrow Fe^{2+} + O_2H^+ \tag{9.8}$$

302 However, in the 1990s, it was shown that the process can be accelerated by irradiation

303 with UV or visible light of wavelengths below 580 nm, and this was investigated as a

304 novel method for water treatment[68,69]. This process, known as photo-Fenton, leads to

305 much faster rates of $HO^\bullet$ generation because the light absorption of $Fe^{3+}$ complexes,

306 which are reduced to $Fe^{2+}$ complexes, produces an extra $HO^\bullet$ and allows the iron cycle

307 to restart without the need for further addition of iron, thus increasing the efficiency of

308 the process[67](Figure 9.5).

$$Fe^{3+}(L)_n + hv \rightarrow Fe^{2+}(L)_{n-1} + L_{ox}^\bullet \tag{9.9}$$

309
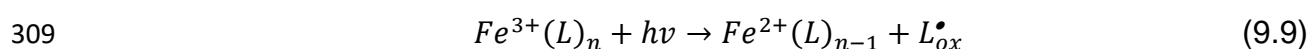
310 This reaction is beneficial for the photo-Fenton process as reduced iron can react with

311 $H_2O_2$ to produce more $HO^\bullet$ (reaction 9.6). However, generation of the radical by

312 reaction 9.6 produces large stoichiometric quantities of $Fe^{3+}$ that precipitate as ferric

313 oxyhydroxides when the pH varies from acid to neutral (the optimal pH to prevent iron

314 precipitation is 2.8)[70,71]. The precipitation of oxyhydroxides reduces the efficiency of

315 the photo-Fenton process[67]. The $Fe^{3+}$ complexes usually generated in acid solution

316 are $Fe(OH)^{2+}$ and $[Fe_2(OH)_2]^{4+}$, which absorb UV or visible light. These complexes

317 undergo photoreduction to yield $HO^\bullet$ and $Fe^{2+}$ (reaction 9.10). The most important iron

318 species in the photo-Fenton process is the $Fe(OH)^{2+}$ complex due to the combination

319 of a high coefficient of absorption and greater concentration relative to $Fe^{3+}$ species.

$$Fe(OH)^{2+} + hv \rightarrow Fe^{2+} + HO^\bullet \tag{9.10}$$

320
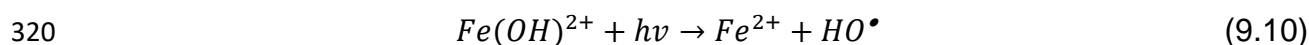
321 [Insert Figure 9.5 here]

322 The first demonstration of the capability of the photo-Fenton process to disinfect water

323 was reported by Rincón and Pulgarin [72]. These authors showed that the use of low

324 concentrations of reagent (0.3 mg/L of Fe and 10 mg/L of $H_2O_2$) greatly enhanced the

325 inactivation kinetics of *E. coli* in water. Since then, the efficiency of the photo-Fenton

process against other pathogens and the related chemical and biological parameters have been investigated using several iron compounds and concentrations, different ratios of $Fe^{2+}/H_2O_2$ or $Fe^{3+}/H_2O_2$, pH values and diverse types of water (DW, MilliQ water, simulated and real municipal WWTP effluents) under simulated and natural solar conditions[73-79].

Nevertheless, the data related to the evaluation of the photo-Fenton process against the protozoan parasite *Cryptosporidium* is very scarce, being non-existent for *Giardia*. The potential improvement of the efficacy of the solar water disinfection against *C. parvum* by the addition of $H_2O_2$ to natural ferruginous waters (NFW) was evaluated in polyethylene terephthalate (PET) bottles of 333 mL and 1.5 L under simulated and natural solar radiation, respectively, at concentrations of 3.4 and 0.3 mg/L of dissolved iron and 0, 10, 50 and 100 mg/L of $H_2O_2$. Under simulated sunlight, a significant lower percentage of viable oocysts was observed in samples of NTW containing 3.4 mg/L of dissolved iron and 100 m/L of $H_2O_2$, in comparison with other concentrations of $H_2O_2$. However, these differences were not observed when the NFW was diluted (0.3 mg/L), observing oocyst viabilities similar to those determined in DW[80]. Nevertheless, under natural solar radiation and using NFW with a concentration of dissolved iron of 0.3 mg/L and $H_2O_2$ concentrations of 0, 10, 50 and 100 mg/L, a strong decrease in the oocyst viability was observed in samples containing 100 mg/L of $H_2O_2$, being significantly lower than the corresponding values detected in the samples containing 0, 10 and 50 mg/L of $H_2O_2$, and, therefore, proving the enhancement in the effectiveness of the solar water disinfection by the addition of $H_2O_2$ to NFW[81].

A further study evaluated the effect of the photo-Fenton process on the survival of *Cryptosporidium* using a factorial 3×3 first order design to study the combined effects of the $Fe^{2+}/H_2O_2$ concentration (5/10; 10/20 and 20/50 mg/L), pH value (3, 5.5 and 8)

351 and exposure time (2, 4 and 6 h) for inactivating *C. parvum* oocysts in DW under

352 natural solar radiation. The parameters $Fe^{2+}/H_2O_2$ concentration and exposure time,

353 as well as the interaction between pH and $Fe^{2+}/H_2O_2$ concentration had a statistically

354 significant influence on the viability of this waterborne enteropathogen. Reductions in

355 the oocyst viability greater than 90% were reached using concentration of $Fe^{2+}/H_2O_2$

356 of 20/50 mg/L, pH 3 and exposure times of 4 and 6 h[82].

357 **9.3 Ultrasound irradiation**

358 For more than one hundred years, ultrasound technology has been used for numerous

359 applications in several fields[83-89], being a non-photochemical AOPs that can be used

360 alone or in combination with water conventional methods and other AOPs for treating

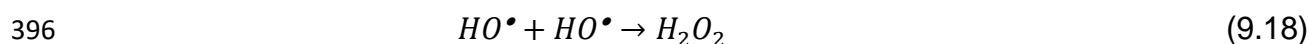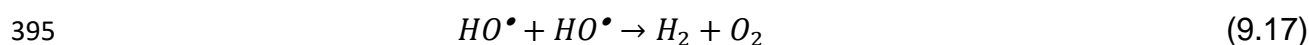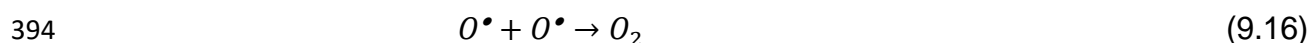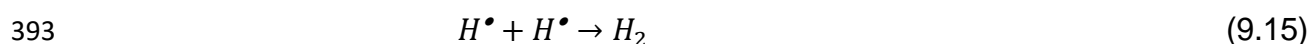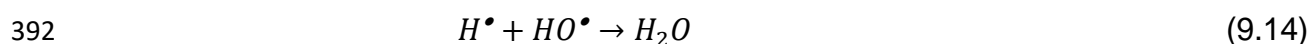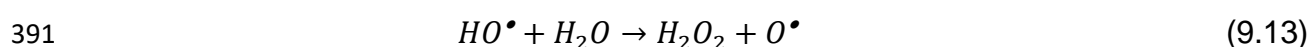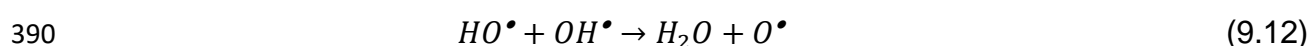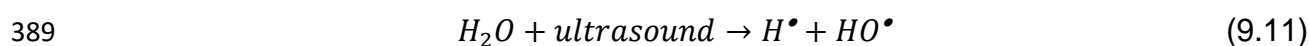361 different types of water, thus increasing the efficacy of disinfection[90-95].

362 Ultrasound comprises sound waves of frequency above the threshold perceived by

363 the human ear (20-20,000 Hz), in a range from 20 kHz to 20 MHz. The waves are

364 generated by mechanical or electrical energy in an ultrasonic transductor and can be

365 classified into different categories depending on their frequency and intensity. Low

366 frequency ultrasound ranges from 20 to 100 kHz, whereas high frequency ultrasound

367 ranges from 100 kHz to 1 MHz. On the other hand, low intensity ultrasound generates

368 power of less than one watt. However, high intensity ultrasound is capable of

369 generating tens of watts.

370 The several applications of ultrasound are based on the phenomenon of acoustic

371 cavitation, which has physical, mechanical and chemical effects on solids as well as

372 in aqueous solutions. In the latter media, the cavitation phenomenon can be

373 differentiated into three successive phases: the first phase consists of the process of

374 nucleation, in which a cavitation core is generated from microbubbles trapped in

375  microfractures of the particles suspended in the aqueous solution; in the second

376  phase, the microbubbles grow and expand depending on the intensity of the sound

377  wave; and, in the final phase of the cavitation process, the microbubbles collapse,

378  although only if the intensity of sound wave exceeds the threshold of acoustic

379  cavitation (usually a few watts per square centimetre at 20 kHz). Under these

380  conditions, the microbubbles expand until they cannot absorb more energy and

381  implode violently. In this phase of collapse, extreme temperature and pressure values

382  are reached, so that the gas trapped inside the microbubble is submitted to molecular

383  fraction, the phenomenon on which sonochemistry is based (Figure 9.6)[96,97].
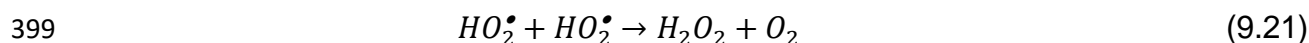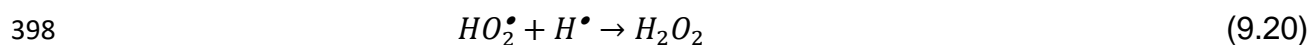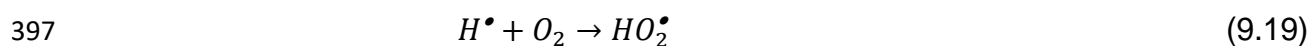
384                    [Insert Figure 9.6 here]

385  The extreme conditions that occur during the collapse of the microbubbles have

386  catalytic effects that lead to various sonochemical reactions. Thus, in pure aqueous

387  systems and as a consequence of the fragmentation of water molecules in the

388  gaseous phase, ROS are generated, in combination with $H_2O_2$ and ozone $(O_3)$[96,98].

389  $$H_2O + ultrasound \rightarrow H^\bullet + HO^\bullet \qquad (9.11)$$

390  $$HO^\bullet + OH^\bullet \rightarrow H_2O + O^\bullet \qquad (9.12)$$

391  $$HO^\bullet + H_2O \rightarrow H_2O_2 + O^\bullet \qquad (9.13)$$

392  $$H^\bullet + HO^\bullet \rightarrow H_2O \qquad (9.14)$$

393  $$H^\bullet + H^\bullet \rightarrow H_2 \qquad (9.15)$$

394  $$O^\bullet + O^\bullet \rightarrow O_2 \qquad (9.16)$$

395  $$HO^\bullet + HO^\bullet \rightarrow H_2 + O_2 \qquad (9.17)$$

396  $$HO^\bullet + HO^\bullet \rightarrow H_2O_2 \qquad (9.18)$$

397
$$H^\bullet + O_2 \rightarrow HO_2^\bullet \tag{9.19}$$

398
$$HO_2^\bullet + H^\bullet \rightarrow H_2O_2 \tag{9.20}$$

399
$$HO_2^\bullet + HO_2^\bullet \rightarrow H_2O_2 + O_2 \tag{9.21}$$

400
$$O_2 \rightarrow 2^\bullet O \tag{9.22}$$

401
$$O_2 + O^\bullet \rightarrow O_3 \tag{9.23}$$
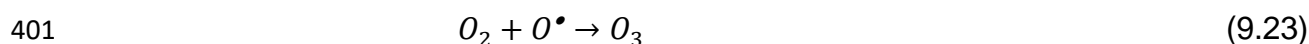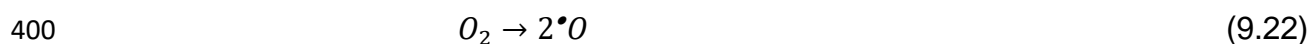
402 The radicals generated react with each other to form new molecules and radicals or

403 they diffuse into the medium, acting as oxidants. In aqueous solutions that contain

404 solutes and organic volatile gas, the collapse of the microbubbles creates $HO^\bullet$ and $H^\bullet$

405 by fragmentation of the water molecules and can also generate inorganic radicals. The

406 production of free radicals and $H_2O_2$ depends on the frequency and intensity of the

407 ultrasound irradiation, the properties of the aqueous solution and the nature of

408 dissolved gas[96].

409 Water treatments based on ultrasound technology have been investigated in relation

410 to the inactivation of different microorganisms using different frequencies and power

411 levels[99,100]. However, studies evaluating the use of ultrasound technology to inactivate

412 *Cryptosporidium* are scarce, varying widely in the type of equipment used and the

413 experimental conditions, with oocyst inactivation rates of 90-95% reported[84,87,91,101].

414 Ashokkumar, et al. [84] applied ultrasound at frequency of 20 kHz and power of

415 approximately 2.5 W in continuous mode to 15 mL samples of Milli-Q water spiked *C.*

416 *parvum* oocysts and showed that more than 90% of *C. parvum* oocysts were not viable

417 after an exposure time of 1.5 min. Oyane, et al. [91] used a murine model and determined

418 an oocyst inactivation of 94.9% after 60 s of ultrasound irradiation at a frequency of

419 27.5 kHz and power of 126 W in 3 mL of saline solution. Olvera, et al. [87] reported

420 oocyst inactivation of 94.0% in 60 mL of water irradiated with ultrasound at higher

421 frequency (1 MHz) at 4.1 W power for 4 min. Finally, Abeledo-Lameiro, et al. [101]

422 evaluated the efficacy of ultrasound technology to inactivate *C. parvum* oocysts at a

423 frequency of 20 kHz and three power levels (60, 80 and 100 W), pulsed at 50% or in

424 continuous mode, in 75 mL samples of four types of water: DW, simulated, real and

425 filtered WWTP effluents, determining reductions of 95-99% in the oocyst viability after

426 the application of ultrasound irradiation at 80 W power in continuous mode for an

427 exposure time of 10 min.

428 Several authors compared pulsed and continuous mode, showing that the use of

429 continuous mode yielded significantly lower values of oocyst viability. This may be due

430 to the existence of a greater number of cavitational events per unit of time in

431 continuous mode relative to pulsed mode. However, considering the *Dose* parameter

432 (energy per volume unit), there are not statistically significant differences in the

433 reductions of the oocyst viability concerning the mode used[84,101].

434 With respect to the water composition, Abeledo-Lameiro, et al. [101] observed higher

435 levels of oocyst inactivation in WWTP effluents than in DW. These differences in the

436 efficacy of ultrasound irradiation may be explained by the variable chemical

437 composition of the samples as dissolved salts and suspended solids increase the

438 action of ultrasound, since they can act as cavitational nuclei[88,102,103]. Even organic

439 matter does not adversely affect, but it may favour the efficacy of ultrasonic

440 disinfection[88,102].

441 Concerning *Giardia,* the data about the elimination of this waterborne protozoan

442 parasite by ultrasound irradiation is more scarce than in the case of *Cryptosporidium.*

443 Marques Passos, et al. [104] evaluated the efficiency of disinfection by ultrasound,

444  individually and in combination with $O_3$, in 1 L effluent of the secondary decanter of a

445  wastewater treatment plant at a frequency of 42 kHz and 100 W. A decrease of 79.2%

446  in the number of *Giardia* spp. cysts was observed after treatment with ultrasound for

447  240 min. When ultrasonic treatment was applied simultaneously with $O_3$ (21 mg/L)

448  reduction of 100% of *Giardia* cysts was determined after 10 min of exposure time[104].

449  Due to the observation of high proportions of partially or totally empty oo/cysts,

450  consequence of a damage to the oo/cyst wall as a result of mechanical fatigue caused

451  by pressure gradients generated by the collapse of the gas microbubbles that enter

452  the solution during acoustic cavitation, most of the authors conclude that the main

453  mechanism of oo/cyst inactivation is the mechanical effect generated during the

454  cavitation events induced by ultrasound[84,91,101,104] (Figure 9.7). Nevertheless, chemical

455  attack due to the formation of free radicals and further recombination of these to form

456  other strong oxidants can also contribute to the oo/cyst inactivation, as the oxidants

457  may alter the chemical structure of the oo/cyst wall and penetrate the cell[86,87].

458                          [Insert Figure 9.7 here]

459

460  **9.4 Adsorption onto granular activated carbon (GAC)**

461  Activated carbon is a group of porous carbons produced by treating charcoal with

462  oxidising gases or by carbonising carbonaceous materials impregnated with

463  dehydrating chemicals. All of them showed a high degree of porosity and a large

464  internal surface area. The use of charcoal has been described as early as 1550 B.C.

465  in Egypt, but it was not until the beginning of the 20th century that commercial

466  production began. The surface of the activated carbon is able to bind molecules from

467  the liquid or gas phase by van der Waals-type physical forces, although chemisorption,

468 caused by stronger valence forces on the so-called active sites of the carbon surface,

469 is also possible[105].

470     In the water industry, activated carbon is mainly used to remove natural organic

471 matter and micro-pollutants or control unpleasant tastes and odour[105]. In the last

472 20 years, the use of activated carbon to remove pathogenic microorganisms from

473 water has been extended. However, few studies carried out at laboratory and pilot

474 scale evaluated the capability of GAC filters, as cartridges or columns, to eliminate

475 *Cryptosporidium* oocysts and *Giardia* cysts from different types of water[106-109].

476     A faucet mounted type water purifier consisting of a cartridge composed of a layer

477 of GAC and a hollow fiber membrane filter with multi-layer pores of 0.1 µm was

478 evaluated against *C. parvum* oocysts. The faucet and the water purifier were

479 connected by an anti-pressure tube, and $3 \times 10^7$ oocyst of *C. parvum* were injected

480 into the tube while the water was running. Any oocyst was found in the purified water

481 collected from all cartridges, showing that the proposed water purifier is effective in

482 removing *C. parvum* oocysts from drinking water[106].

483     The capability of GAC adsorption filters to remove *C. parvum* and *G. duodenalis*

484 oo/cysts seems to be higher in comparison with other pathogens such as viruses and

485 bacteria. In a pilot scale carried out using two duplicate columns (ø = 0.15 m; height

486 1.35 m; median grain size 1 mm) loaded with 1 m of GAC, which were supplied with

487 pre-treated surface water (at constant filtration rate of 5 m/h and contact time of 12

488 min), removal values of 2.7 and 1.3 log were obtained for *C. parvum* oocysts in fresh

489 and loaded GAC, respectively, whereas 2.1 log reductions were observed for

490 *G. duodenalis* cysts in both fresh and loaded GAC. However, MS2 phages were not

491 eliminated from the water and the removal of *E. coli* and spores of *Clostridium*

492 *bifermentans* was limited (≤0.1-1.1 log)[107]. Other study assessed the efficacy of a GAC

biofilter in reducing pathogens using a modified feed-water formulation spiked with a cocktail of five pathogen surrogates (*S. epidermidis*, *E. coli*, *Enterococcus faecalis*, MS2 bacteriophage and *Saccharomyces cerevisiae*) which represent four groups of microbial pathogens (human skin-associated and enteric bacteria, human enteric viruses and *Cryptosporidium* and *Giardia* oo/cysts). The system showed a range of removal efficiencies towards five surrogates, although the highest reduction occurred with the surrogate for *Cryptosporidium* and *Giardia*: no reduction for MS2 virus; 0.3 log reductions for *E. coli*; 0.9 log reductions for *E. faecalis*; 1.1 log reductions for *S. epidermidis*; and, 3.4 log reductions for S. *cerevisiae*[109].

Another point to consider in the removal of waterborne protozoan parasites by GAC is the age and/or saturation of the filter since several studies suggest that these parameters can enhance the retention of *Cryptosporidium* oocysts and *Giardia* cysts. Thus, loaded GAC showed higher concentrations of retained parasitic forms than the fresh GAC, being especially remarkable for *C. parvum* oocysts[107], and high efficiencies of removal correlate well with the degree of biofilm development[108]. Moreover, a study demonstrated log reductions of 0.7 and 2.7 for *S. cerevisiae* (used as a surrogate for *Cryptosporidium* and *Giardia*) in unsaturated and saturated zones of a GAC biofilter[109].

On the other hand, eukaryotic organisms are ubiquitous in surface waters, and some species can proliferate in granular filters of water treatment plants and colonize distribution systems. Also, it is known that some waterborne pathogens can maintain their viability inside other organisms, obtaining the protection of a structure that allows its transport and persistence through water systems[110-115]. Although the role of most zooplankton organisms (rotifers, copepods, cladocerans) in pathogen transmission through drinking water remains poorly understood, some authors have questioned if predation by zooplankton has an impact on the transport and fate of *Cryptosporidium*

518   and *Giardia* oo/cysts in GAC filters[116,117]. In a pilot plant study carried out with two

519   parallel GAC filter columns (ø = 15 cm; 1 m deep; 5 m/h; contact time of 12 min; and

520   no back washing), which operated under full scale conditions, an average mass

521   reduction of *C. parvum* oocysts of 66.2% and 32.1% was observed after two weeks in

522   the upper (0-30 cm) and lower (50-95 cm) parts of the GAC filter beds, respectively[116].

523   In the case of *G. duodenalis* cysts, a slight mass reduction was determined after one

524   week, which was not significant as consequence of the large variations observed in

525   cyst concentrations. Zooplankton was isolated from the filter bed and effluent water,

526   which was enumerated and identified, revealing that rotifers[116], predators of

527   oo/cysts[110-112], were the major part of the isolated zooplankton. Associated with this

528   zooplankton, *C. parvum* oocysts and *G. duodenalis* cysts were detected at average

529   concentrations ranging from 1-12 oocysts/mL and 10-86 cysts/mL, respectively,

530   concluding that predation by zooplankton can have an effect on the remobilization of

531   *Cryptosporidium* and *Giardia* oo/cysts retained in GAC filter beds and, therefore, in the

532   transmission of these protozoa in drinking water[116]. However, a further study

533   demonstrated that under best-practice operating conditions of drinking water

534   treatment plants, internalized *C. parvum* and *G. duodenalis* oo/cysts are unlikely to be

535   a major concern to the water industry[117].

536

537   **9.5. Concluding remarks**

538   Studies evaluating the efficacy of photocatalytic AOPs, ultrasound and GAC filters

539   against the waterborne protozoan parasites *Cryptosporidium* and *Giardia* are scarce.

540   Among them, most studies assessed the inactivation of *C. parvum*, probably because

541   *C. parvum* oocysts are more resistant than *G. duodenalis* cysts. In this way, *C. parvum*

542   is considered as by the World Health Organization (WHO) as a reference organism

543    for protozoan pathogens in the validation of water treatments[118]. Furthermore, given

544    the robust nature of oocysts, inactivation of *Cryptosporidium* would probably ensure

545    the elimination of other less resistant pathogens.

546    Several studies showed the effectiveness of $TiO_2$ solar photocatalysis in the

547    inactivation of *C. parvum* oocysts in DW, being higher when $TiO_2$ slurry is used.

548    However, the presence of chlorides, phosphates, carbonates and bicarbonates in

549    water affect negatively the efficiency of the process. Taking into account the diversity

550    of types of water, further studies are needed to optimize the employ of $TiO_2$

551    photocatalysis and to evaluate doped $TiO_2$ formulations against these

552    enteropathogens.

553    Only three studies carried out by the same research team evaluated the efficiency of

554    the photo-Fenton process against *C. parvum* oocysts in DW and NFW under simulated

555    and natural solar conditions. Therefore, more studies are required to assess the

556    influence of different factors such as the water matrix, pH, intensity of the radiation

557    and presence of chelates in the inactivation of *Cryptosporidium* and *Giardia* by photo-

558    Fenton processes.

559    Because of both the physical effects of acoustic cavitation and the chemical effects of

560    the $HO^{\bullet}$ generated, ultrasound irradiation is a promising alternative to the disinfection

561    methods currently used in water, without changing the chemical composition of the

562    water or producing toxic by-products. Moreover, ultrasonic treatment that can be used

563    alone or in combination with water conventional methods and other AOPs for treating

564    different types of water, thus increasing the efficacy of disinfection. However, more

565    studies combining ultrasound and conventional water disinfection methods and other

566 AOPs in the inactivation of waterborne protozoan parasites should be carried out, as

567 the related data is very scarce.

568 Unlike for viruses and bacteria, GAC adsorption filters can constitute important barriers

569 for *Cryptosporidium* and *Giardia* oo/cysts in water treatment. Aged GAC filters seem

570 to be more efficient to retain parasitic forms, demonstrating the important role of

571 biofilms. Although attachment of protozoan oo/cysts appeared to be the dominant

572 removal mechanism in the GAC filters, further studies are needed to confirm this, to

573 assess the potential effects on oo/cyst viability and to evaluate the influence of GAC

574 type and back washing on the removal capability of full-scale GAC adsorption filters.

575 **ABBREVIATIONS**

576 AOPs: Advanced oxidation processes

577 B.C.: Before Christ

578 CPCs: Compound parabolic collectors

579 CT: Contact time

580 DW: Distilled water

581 GAC: Granular activated carbon

582 NFW: Natural ferruginous water

583 PET: Polyethylene terephthalate

584 PV: Parasitophorous vacuole

585 ROS: Reactive oxigen species

586 UV: Ultraviolet

587 WHO: World Health Organization

588 WWTP: Wastewater treatment plant

589

590 **ACKNOWLEDGEMENTS**

600 **References**

601 1. S. M. Cacciò, in *Zoonoses: infections affecting humans and animals*, ed. A.

602 Sing, Springer, Heidelberg, 2015.

603 2. S. M. Cacciò and L. Putignani, in Cryptosporidium*: parasite and disease*, eds.

604 S. M. Cacciò and A. Widmer, Springer Science & Business Media, Vienna,

605 2014.

606 3. S. Dong, Y. Yang, Y. Wang, D. Yang, Y. Yang, Y. Shi, C. Li, L. Li, Y. Chen, Q.

607 Jiang and Y. Zhou, *Acta Parasitol.*, 2020, **65**, 882.

608 4. S. Baldursson and P. Karanis, *Water Res.*, 2011, **45**, 6603.

609 5. A. Efstratiou, J. E. Ongerth and P. Karanis, *Water Res.*, 2017, **114**, 14.

610 6. P. Karanis, C. Kourenti and H. Smith, *J. Water Health*, 2007, **5**, 1.

611   7.    J. Y. Ma, M. Y. Li, Z. Z. Qi, M. Fu, T. F. Sun, H. M. Elsheikha and W. Cong, *Sci.*

612         *Total Environ.*, 2022, **806**, 150562.

613   8.    U. M. Ryan, Y. Feng, R. Fayer and L. Xiao, *Int. J. Parasitol.*, 2021, **51**, 1099.

614   9.    R. Fayer and L. Xiao, Cryptosporidium *and cryptosporidiosis*, CRC Press, Boca

615         Raton, 2008.

616   10.    R. M. Chalmers, A. P. Davies and K. Tyler, *Microbiology*, 2019, **165**, 500.

617   11.    A. Zahedi and U. Ryan, *Res. Vet. Sci.*, 2020, **132**, 500.

618   12.    W. L. Current and L. S. García, *Clin. Microbiol. Rev.*, 1991, **4**, 325.

619   13.    M. Bouzid, P. R. Hunter, R. M. Chalmers and K. M. Tyler, *Clin. Microbiol. Rev.*,

620         2013, **26**, 115.

621   14.    P. J. O'Donoghue, *Int. J. Parasitol.*, 1995, **25**, 139.

622   15.    S. Tzipori and J. K. Griffiths, *Adv. Parasitol.*, 1998, **40**, 5.

623   16.    S. Tzipori and H. Ward, *Microbes Infect.*, 2002, **4**, 1047.

624   17.    D. H. Hill and T. Nash, in *Tropical infectious diseases. Principles, pathogens*

625         *and practice*, eds. R. Guerrant, D. Krogstad, J. Maquire, J. Walker and P.

626         Weller, Churchill Livingston, Filadelfia, 2011.

627   18.    R. C. A. Thompson, in *Zoonoses*, eds. S. R. Palmer, E. J. Soulsby, P.

628         Torgerson and D. Brown, Oxford University Press, Oxford, 2011.

629   19.    R. D. Adam, *Clin. Microbiol. Rev.*, 2001, **14**, 447.

630   20.    K. A. Hamilton, M. Waso, B. Reyneke, N. Saeidi, A. Levine, C. Lalancette, M.

631         C. Besner, W. Khan and W. Ahmed, *J. Environ. Qual.*, 2018, **47**, 1006.

632   21.    J. Lu, H. Ryu, S. Hill, M. Schoen, N. Ashbolt, T. A. Edge and J. S. Domingo,

633         *Water Res.*, 2011, **45**, 3960.

634   22.    W. Ahmed, T. Sritharan, A. Palmer, J. P. Sidhu and S. Toze, *Appl. Environ.*

635         *Microbiol.*, 2013, **79**, 2682.

636    23.    J. P. Sidhu, W. Ahmed, W. Gernjak, R. Aryal, D. McCarthy, A. Palmer, P.

637           Kolotelo and S. Toze, *Sci. Total Environ.*, 2013, **463-464**, 488.

638    24.    W. Ahmed, A. Goonetilleke and T. Gardner, *Water Res.*, 2010, **44**, 4662.

639    25.    C. L. Schneeberger, M. O'Driscoll, C. Humphrey, K. Henry, N. Deal, K. Seiber,

640           V. R. Hill and M. Zarate-Bermudez, *J. Environ. Health*, 2015, **77**, 22.

641    26.    L. C. Vermeulen, M. van Hengel, C. Kroeze, G. Medema, J. E. Spanier, M. T.

642           H. van Vliet and N. Hofstra, *Water Res.*, 2019, **149**, 202.

643    27.    G. J. Medema and J. F. Schijven, *Water Res.*, 2001, **35**, 4307.

644    28.    N. Hofstra and L. C. Vermeulen, *Int. J. Hyg. Environ. Health.*, 2016, **219**, 599.

645    29.    D. Kanakaraju, B. D. Glass and M. Oelgemoller, *J. Environ. Manage.*, 2018,

646           **219**, 189.

647    30.    J. H. Carey, J. Lawrence and H. M. Tosine, *Bull. Environ. Contam. Toxicol.*,

648           1976, **16**, 697.

649    31.    J. M. Herrmann, *Top. Catal.*, 2005, **34**, 49.

650    32.    S. Malato, P. Fernández-Ibáñez, M. I. Maldonado, J. Blanco and W. Gernjak,

651           *Catal. Today*, 2009, **147**, 1.

652    33.    J. A. Byrne, P. S. Dunlop, J. W. Hamilton, P. Fernández-Ibáñez, I. Polo-López,

653           P. K. Sharma and A. S. Vennard, *Molecules*, 2015, **20**, 5574.

654    34.    P. Fernández-Ibáñez, J. Blanco, S. Malato and F. J. de las Nieves, *Water Res.*,

655           2003, **37**, 3180.

656    35.    W. Xi and S. U. Geissen, *Water Res.*, 2001, **35**, 1256.

657    36.    J. Gustafsson, E. Nordenswan and J. B. Rosenholm, *J. Colloid Interface Sci.*,

658           2003, **258**, 235.

659    37.    R. Thiruvenkatachari, S. Vigneswaran and I. S. Moon, *Korean J. Chem. Eng.*,

660           2008, **25**, 64.

661    38.    M. N. Chong, B. Jin, C. W. Chow and C. Saint, *Water Res.*, 2010, **44**, 2997.

662    39.    H. A. Foster, I. B. Ditta, S. Varghese and A. Steele, *Appl. Microbiol. Biotechnol.*,

663         2011, **90**, 1847.

664    40.    L. W. Gassie and J. D. Englehardt, *Water Res.*, 2017, **125**, 384.

665    41.    T. Matsunaga, R. Tomoda, T. Nakajima and H. Wake, *FEMS Microbiol. Lett.*,

666         1985, **29**, 211.

667    42.    J. C. Ireland, P. Klostermann, E. W. Rice and R. M. Clark, *Appl. Environ.*

668         *Microbiol.*, 1993, **59**, 1668.

669    43.    J. A. Herrera Melián, J. M. Dona Rodríguez, A. Viera Suárez, E. Tello Rendón,

670         C. Valdés do Campo, J. Arana and J. Pérez Pena, *Chemosphere*, 2000, **41**,

671         323.

672    44.    A.-G. Rincón and C. Pulgarin, *Sol. Energy*, 2004, **77**, 635.

673    45.    O. Seven, B. Dindar, S. Aydemir, D. Metin, M. A. Ozinel and S. Icli, *J.*

674         *Photochem. Photobiol. A-Chem.*, 2004, **165**, 103.

675    46.    C. Sichel, M. de Cara, J. Tello, J. Blanco and P. Fernández-Ibáñez, *Appl. Catal.*

676         *B-Environ.*, 2007, **74**, 152.

677    47.    M. I. Polo-López, P. Fernández-Ibáñez, I. García-Fernández, I. Oller, I.

678         Salgado-Tránsito and C. Sichel, *J. Chem. Technol. Biotechnol.*, 2010, **85**, 1038.

679    48.    A. M. Nasser, *J. Water Health*, 2016, **14**, 1.

680    49.    M. Otaki, T. Hirata and S. Ohgaki, *Water Sci. Technol.-Water Supply*, 2000, **42**,

681         103.

682    50.    T. P. Curtis, G. Walker, B. M. Dowling and P. A. Christensen, *Water Res.*, 2002,

683         **36**, 2410.

684    51.    J. H. Lee, M. Kang, S. J. Choung, K. Ogino, S. Miyata, M. S. Kim, J. Y. Park

685         and J. B. Kim, *Water Res.*, 2004, **38**, 713.

686    52.    F. Méndez-Hermida, E. Ares-Mazás, K. G. McGuigan, M. Boyle, C. Sichel and

687            P. Fernández-Ibáñez, *J. Photochem. Photobiol. B-Biol.*, 2007, **88**, 105.

688    53.    M. Cho and J. Yoon, *J. Appl. Microbiol.*, 2008, **104**, 759.

689    54.    H. Ryu, D. Gerrity, J. C. Crittenden and M. Abbaszadegan, *Water Res.*, 2008,

690            **42**, 1523.

691    55.    M. Sokmen, S. Degerli and A. Aslan, *Exp. Parasitol.*, 2008, **119**, 44.

692    56.    S. Navalon, M. Alvaro, H. Garcia, D. Escrig and V. Costa, *Water Sci. Technol.*,

693            2009, **59**, 639.

694    57.    O. Sunnotel, R. Verdoold, P. S. Dunlop, W. J. Snelling, C. J. Lowery, J. S.

695            Dooley, J. E. Moore and J. A. Byrne, *J. Water Health*, 2010, **8**, 83.

696    58.    M. Fontán Sainz, PhD Thesis, University of Santiago de Compostela, 2012.

697    59.    M. J. Abeledo-Lameiro, E. Ares-Mazás and H. Gómez-Couso, *J. Photochem.*

698            *Photobiol. B-Biol.*, 2016, **163**, 92.

699    60.    M. J. Abeledo-Lameiro, A. Reboredo-Fernández, M. I. Polo-López, P.

700            Fernández-Ibáñez, E. Ares-Mazás and H. Gómez-Couso, *Catal. Today*, 2017,

701            **280**, 132.

702    61.    C. Pablos, J. Marugán, R. van Grieken and E. Serrano, *Water Res.*, 2013, **47**,

703            1237.

704    62.    E. Unosson, E. K. Tsekoura, H. Engqvist and K. Welch, *Biomatter*, 2013, **3**.

705    63.    O. K. Darlrymple, E. Stefanakos, M. A. Trotz and D. Y. Goswami, *Appl. Catal.*

706            *B*, 2010, **98**, 27.

707    64.    K. G. McGuigan, F. Méndez-Hermida, J. A. Castro-Hermida, E. Ares-Mazás, S.

708            C. Kehoe, M. Boyle, C. Sichel, P. Fernández-Ibáñez, B. P. Meyer, S.

709            Ramalingham and E. A. Meyer, *J. Appl. Microbiol.*, 2006, **101**, 453.

710    65.    H. Fenton, *J. Chem. Soc.-Trans.*, 1894, **65**, 899.

711 66. F. Haber and J. Weiss, *Proc. R. Soc. London Ser. A-Math. Phys. Sci.*, 1934,

712 **147**, 332.

713 67. J. J. Pignatello, E. Oliveros and A. MacKay, *Crit. Rev. Environ. Sci. Technol.*,

714 2006, **36**, 1.

715 68. R. Bauer, *Chemosphere*, 1994, **29**, 1225.

716 69. T. Oppenländer, *Photochemical purification of water and air. Principles,*

717 *reaction mechanisms and reactor concepts*, Wiley, Weinheim, 2003.

718 70. W. Tang and C. Huang, *Environ. Technol.*, 1996, **17**, 1371.

719 71. B. G. Kwon, D. S. Lee, N. Kang and J. Yoon, *Water Res.*, 1999, **33**, 2110.

720 72. A. G. Rincón and C. Pulgarin, *Appl. Catal. B-Environ.*, 2006, **63**, 222.

721 73. F. Sciacca, J. A. Rengifo-Herrera, J. Wethe and C. Pulgarin, *Chemosphere*,

722 2010, **78**, 1186.

723 74. E. R. Bandala, L. González, J. L. Sánchez-Salas and J. H. Castillo, *J. Water*

724 *Health*, 2012, **10**, 20.

725 75. E. Ortega-Gómez, P. Fernández-Ibáñez, M. M. Ballesteros Martín, M. I. Polo-

726 López, B. Esteban García and J. A. Sánchez Pérez, *Water Res.*, 2012, **46**,

727 6154.

728 76. M. I. Polo-López, I. García-Fernández, T. Velegraki, A. Katsoni, I. Oller, D.

729 Mantzavinos and P. Fernández-Ibáñez, *Appl. Catal. B-Environ.*, 2012, **111-112**,

730 545.

731 77. M. I. Polo-López, I. Oller and P. Fernández-Ibáñez, *Catal. Today*, 2013, **209**,

732 181.

733 78. D. Polo, I. García-Fernández, P. Fernández-Ibáñez and J. L. Romalde, *Food*

734 *Environ. Virol.*, 2018, **10**, 159.

735 79. I. García-Fernández, S. Miralles-Cuevas, I. Oller, S. Malato, P. Fernández-
736 Ibáñez and M. I. Polo-López, *J. Hazard. Mater.*, 2019, **372**, 85.

737 80. A. Reboredo-Fernández, M. J. Abeledo-Lameiro, E. Ares-Mazás and H.
738 Gómez-Couso, The 13th IWA Leading Edge Conference on Water and
739 Wastewater Technologies, Jérez de la Frontera, 13-16 June, 2016.

740 81. A. Reboredo-Fernández, M. J. Abeledo-Lameiro, I. Polo-López, P. Fernández-
741 Ibáñez, E. Ares-Mazás and H. Gómez-Couso, The 13th IWA Leading Edge
742 Conference on Water and Wastewater Technologies, Jérez de la Frontera, 13-
743 16 June, 2016.

744 82. M. J. Abeledo-Lameiro, M. I. Polo-López, E. Ares-Mazás and H. Gómez-Couso,
745 *Appl. Catal. B-Environ.*, 2019, **253**, 341.

746 83. L. Thompson and L. Doraiswamy, *Ind. Eng. Chem. Res.*, 1999, **38**, 1215.

747 84. M. Ashokkumar, T. Vu, F. Grieser, A. Weerawardena, N. Anderson, N.
748 Pilkington and D. R. Dixon, *Water Sci. Technol.*, 2003, **47**, 173.

749 85. P. Piyasena, E. Mohareb and R. C. McKellar, *Int. J. Food Microbiol.*, 2003, **87**,
750 207.

751 86. A. Antoniadis, I. Poulios, E. Nikolakaki and D. Mantzavinos, *J. Hazard. Mater.*,
752 2007, **146**, 492.

753 87. M. Olvera, A. Eguia, O. Rodríguez, E. Chong, S. D. Pillai and K. Ilangovan,
754 *Bioresour. Technol.*, 2008, **99**, 2046.

755 88. S. Drakopoulou, S. Terzakis, M. S. Fountoulakis, D. Mantzavinos and T.
756 Manios, *Ultrason. Sonochem.*, 2009, **16**, 629.

757 89. J. Wang, Y. Guo, B. Liu, X. Jin, L. Liu, R. Xu, Y. Kong and B. Wang, *Ultrason.*
758 *Sonochem.*, 2011, **18**, 177.

759 90. T. Blume and U. Neis, *Ultrason. Sonochem.*, 2004, **11**, 333.

760  91.  I. Oyane, M. Furuta, C. E. Stavarache, K. Hashiba, S. Mukai, J. M. Nakanishi,

761      I. Kimata and Y. Maeda, *Environ. Sci. Technol.*, 2005, **39**, 7294.

762  92.  V. Naddeo, M. Landi, V. Belgiorno and R. M. Napoli, *J. Hazard. Mater.*, 2009,

763      **168**, 925.

764  93.  A. M. Al-Hashimi, T. J. Mason and E. M. Joyce, *Environ. Sci. Technol.*, 2015,

765      **49**, 11697.

766  94.  Z. Wei, R. Spinney, R. Ke, Z. Yang and R. Xiao, *Environ. Chem. Lett.*, 2016,

767      **14**, 163.

768  95.  J. Madhavan, J. Theerthagiri, D. Balaji, S. Sunitha, M. Y. Choi and M.

769      Ashokkumar, *Molecules*, 2019, **24**, 3341.

770  96.  N. Ince, G. Tezcanli, R. Belen and İ. G. Apikyan, *Appl. Catal. B-Environ.*, 2011,

771      **29**, 167.

772  97.  M. Zupanc, Z. Pandur, T. Stepisnik Perdih, D. Stopar, M. Petkovsek and M.

773      Dular, *Ultrason. Sonochem.*, 2019, **57**, 147.

774  98.  Y. G. Adewuyi, *Environ. Sci. Technol.*, 2005, **39**, 3409.

775  99.  S. Gao, G. D. Lewis, M. Ashokkumar and Y. Hemar, *Ultrason. Sonochem.*,

776      2014, **21**, 454.

777  100. J. Li, J. Ahn, D. Liu, S. Chen, X. Ye and T. Ding, *Appl. Environ. Microbiol.*, 2016,

778      **82**, 1828.

779  101. M. J. Abeledo-Lameiro, E. Ares-Mazás and H. Gómez-Couso, *Ultrason.*

780      *Sonochem.*, 2018, **48**, 118.

781  102. B. A. Madge and J. N. Jensen, *Water Environ. Res.*, 2002, **74**, 159.

782  103. P. R. Gogate, *Chem. Eng. Process.*, 2008, **47**, 515.

783   104.   T. Marques Passos, L. H. Moreira da Silva, L. Marmo Moreira, R. Amaro

784          Zângaro, R. da Silva Santos, F. Barrinha Fernandes, C. José de Lima and A.

785          Barrinha Fernandes, *Ozone-Sci. Eng.*, 2014, **36**, 138.

786   105.   H. Marsh and F. Rodríguez-Reinoso, *Activated carbon*, Elsevier Ltd., Oxford,

787          2006.

788   106.   T. Matsui, J. Kajima and T. Fujino, *J. Vet. Med. Sci.*, 2004, **66**, 941.

789   107.   W. A. Hijnen, G. M. Suylen, J. A. Bahlman, A. Brouwer-Hanzens and G. J.

790          Medema, *Water Res.*, 2010, **44**, 1224.

791   108.   I. Papineau, N. Tufenkji, P. Servais and B. Barbeau, *J. Environ. Eng.*, 2012,

792          **139**, 603.

793   109.   A. Sharaf, B. Guo, D. C. Shoults, N. J. Ashbolt and Y. Liu, *Sustainability*, 2020,

794          **12**, 8847.

795   110.   R. Fayer, J. M. Trout, E. Walsh and R. Cole, *J. Eukaryot. Microbiol.*, 2000, **47**,

796          161.

797   111.   J. M. Trout, E. J. Walsh and R. Fayer, *J. Parasitol.*, 2002, **88**, 1038.

798   112.   R. Stott, E. May, E. Ramírez and A. Warren, *Water Sci. Technol.*, 2003, **47**, 77.

799   113.   F. Méndez-Hermida, H. Gómez-Couso and E. Ares-Mazás, *J. Eukaryot.*

800          *Microbiol.*, 2006, **53**, 432.

801   114.   H. Gómez-Couso, E. Paniagua-Crespo and E. Ares-Mazás, *Parasitol. Res.*,

802          2007, **100**, 1151.

803   115.   F. Bichai, P. Payment and B. Barbeau, *Can. J. Microbiol.*, 2008, **54**, 509.

804   116.   F. Bichai, B. Barbeau, Y. Dullemont and W. Hijnen, *Water Res.*, 2010, **44**, 1072.

805   117.   F. Bichai, Y. Dullemont, W. Hijnen and B. Barbeau, *Water Res.*, 2014, **64**, 296.

806   118.   World Health Organization, *Guidelines for drinking-water quality: fourth edition*

807          *incorporating the first addendum*, World Health Organization, Geneva, 2017.

808  119.  M. J. Abeledo Lameiro, PhD Thesis, University of Santiago de Compostela,

809       2020.

810  120.  M. Ruiz Villarreal, *Life cycle of the parasite Giardia lamblia*, 2021. Available

811       from       https://commons.wikimedia.org/wiki/File:Giardia_life_cycle_en.svg.

812       Accessed: April 4th, 2022.

813

814  **FIGURE CAPTIONS**

815  *Figure 9.1 Schematic representation of the life cycle of* Cryptosporidium *species*[119].

816  *Figure 9.2 Schematic representation of the life cycle of* G. duodenalis*.* **Reproduced**

817  **from Ruiz Villarreal [120] under CC0 license.**

818  *Figure 9.3 Diagram illustrating an advanced oxidation process involving the use of UV*

819  *radiation of 300-400 nm in a particle of $TiO_2$ to excite an electron to the conduction*

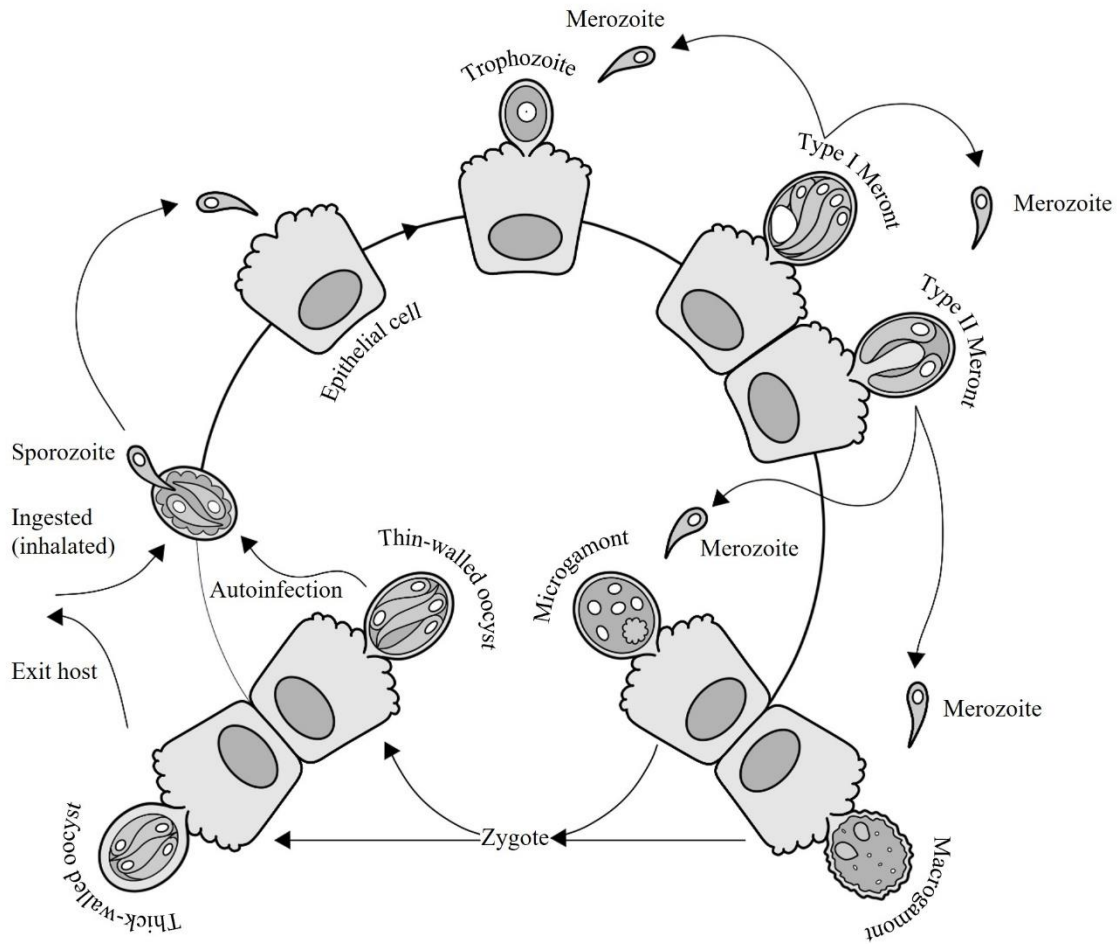820  *band, creating a positive opening in the valence band ($h^+$)*[119]*.*

821  *Figure 9.4 Microphotographs of* C. parvum *oocysts after exposure to simulated solar*

822  *radiation in distilled water containing 0, 63, 100 or 200 mg/L of $TiO_2$. A, D, G and J,*

823  *bright field microscopy; B, E, H and K, direct immunofluorescence antibody technique;*

824  *C, F, I and L, inclusion/exclusion of the fluorogenic vital dye propidium iodide. Bar, 10*

825  *µm.* **Reproduced from Abeledo-Lameiro, et al. [59] with permission from Elsevier,**

826  **Copyright 2022.**

827  *Figure 9.5 Diagram illustrating the attack of hydroxyl radicals ($HO^\bullet$) on the*

828  Cryptosporidium *oocyst wall during photo-Fenton process.* **Reproduced from**

829  **Abeledo-Lameiro, et al. [82] with permission from Elsevier, Copyright 2022.**

830 *Figure 9.6 Representative diagram of the successive phases of the cavitation*

831 *phenomenon[119]. A, ultrasound irradiation of aqueous solution; B, core and growth*

832 *phase of microbubbles of cavitation; C, hot core gas, site where extreme values of*

833 *temperature and pressure are reached; D, interphase or middle region, where a*

834 *temperature gradient occurs; E, aqueous dissolution, with ambient temperature and*

835 *atmospheric pressure values; and, F, collapse of cavitation microbubble. $\tau$, half-life of*

836 *microbubbles of cavitation.*

837 *Figure 9.7 Microphotographs of* C. parvum *oocysts after ultrasonic treatment showing*

838 *numerous empty oocysts. A, direct immunofluorescence antibody technique; B,*

839 *Nomarski interference contrast; C, inclusion/exclusion of the fluorogenic vital dye*
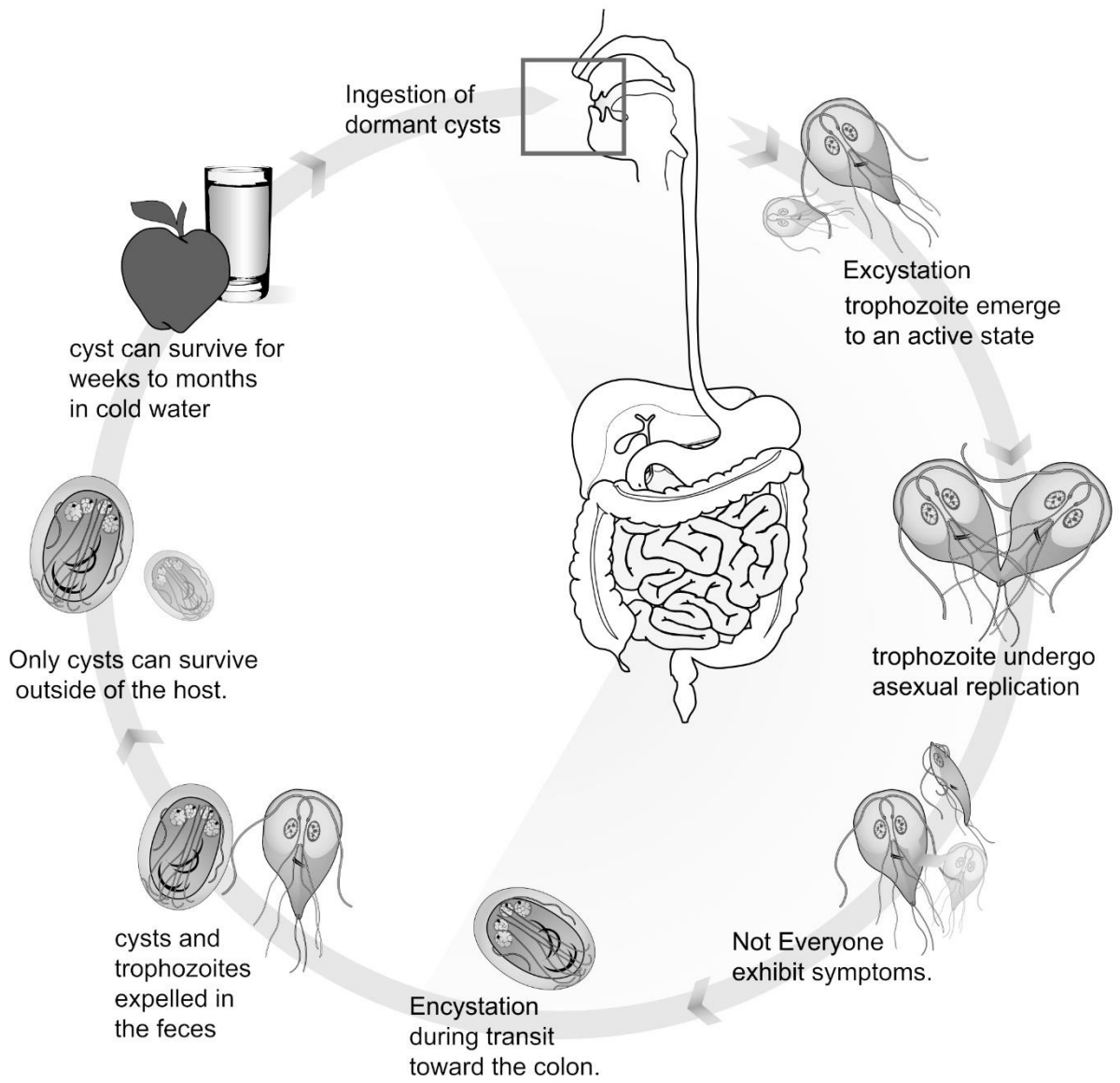
840 *propidium iodide. Bar, 10 μm.*
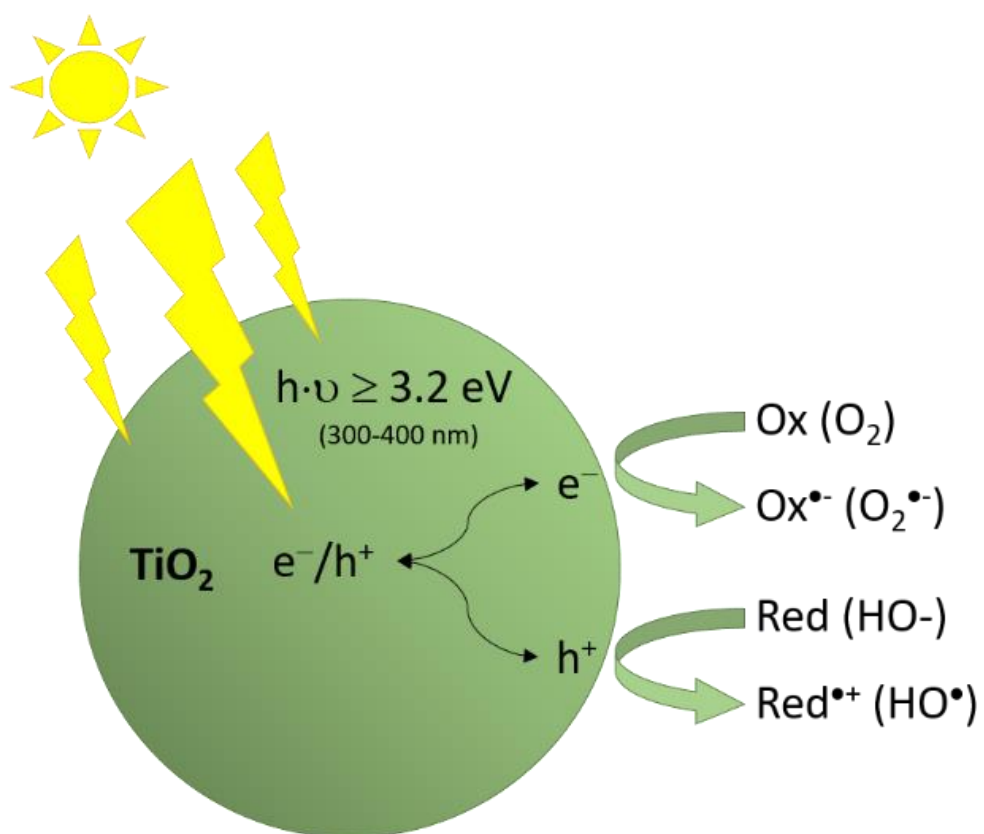
841 **Figure 9.1**



842

843

844     **Figure 9.2**



Ingestion of
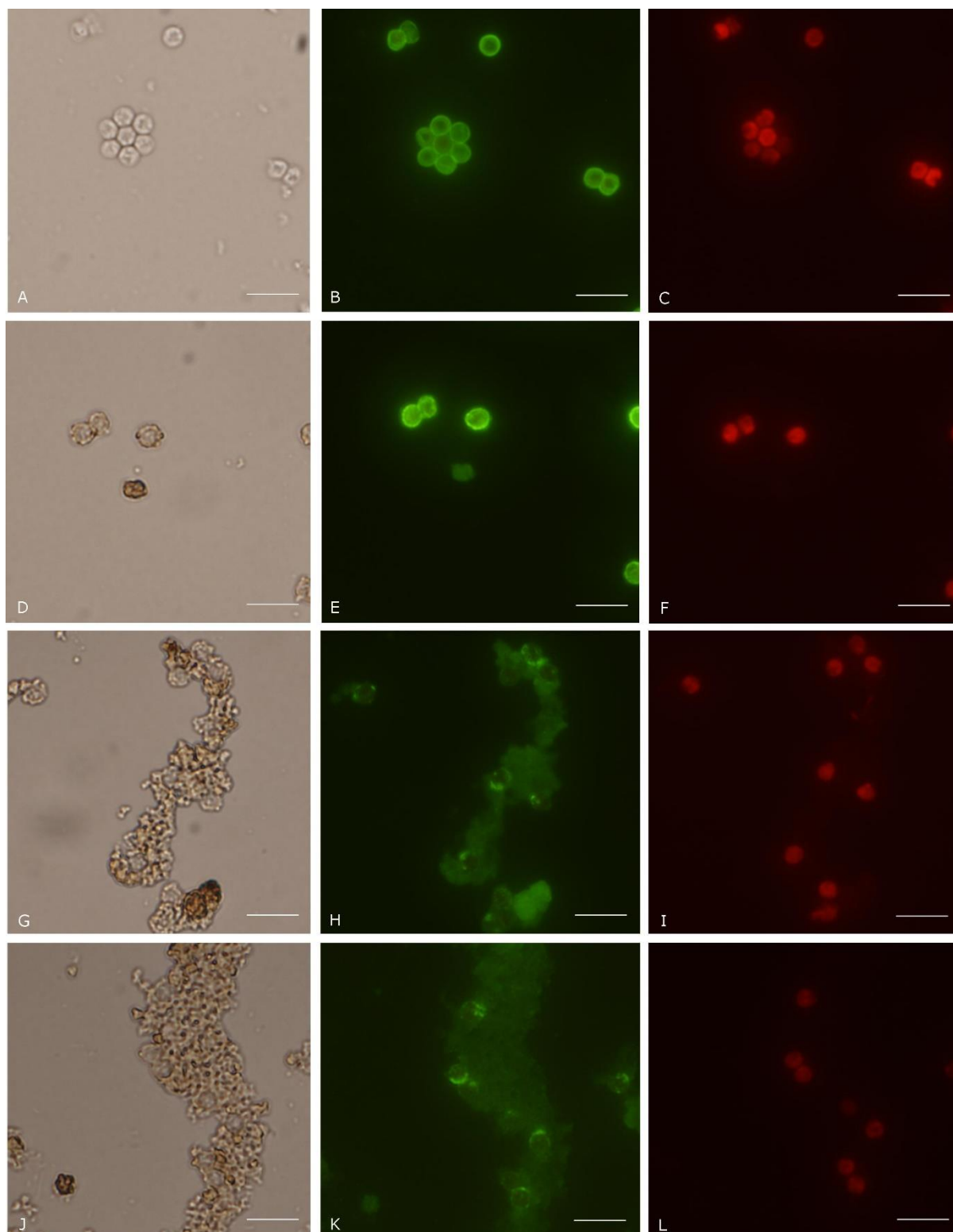dormant cysts

Excystation
trophozoite emerge
to an active state

cyst can survive for
weeks to months
in cold water

trophozoite undergo
asexual replication

Only cysts can survive
outside of the host.

Not Everyone
exhibit symptoms.

cysts and
trophozoites
expelled in
the feces

Encystation
during transit
toward the colon.

845

846

847

848      **Figure 9.3**



849

850

851 **Figure 9.4**

852



853

854

855    **Figure 9.5**



856

857

858

859    **Figure 9.6**



Size ≈ 100-170 μm

B

A

$T \leq 5000\ °C$
$P \leq 500$ atm
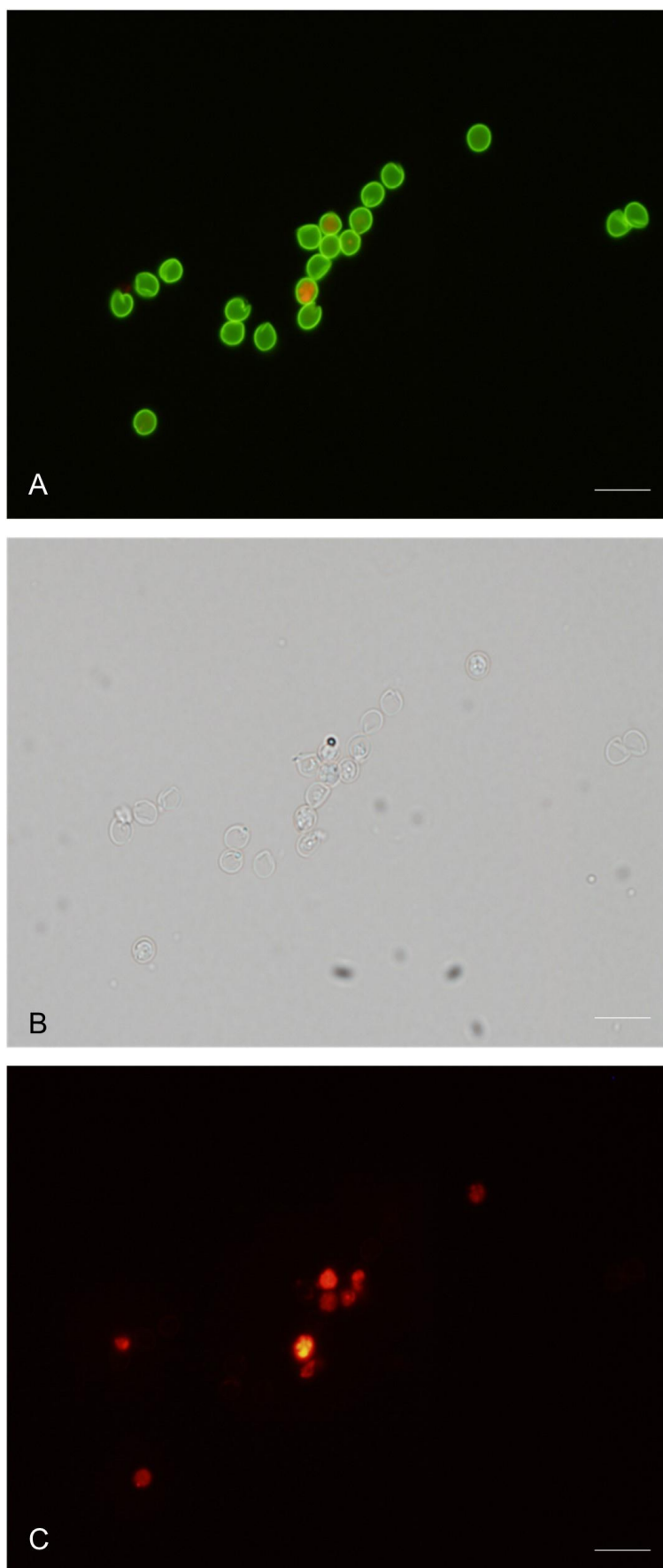
C         D   E          $\tau < 10\ \mu s$

Ambient temperature
Atmospheric pressure

F
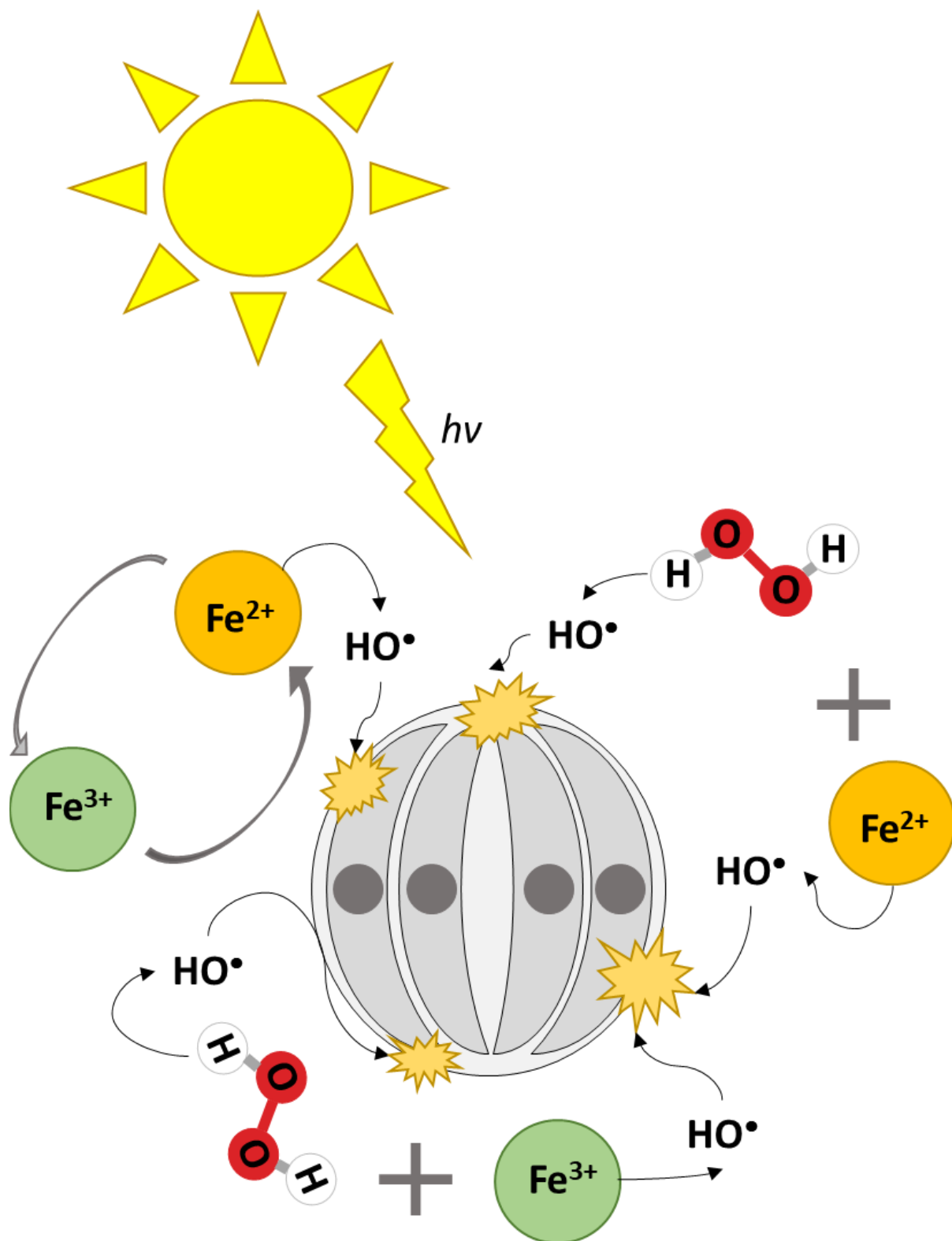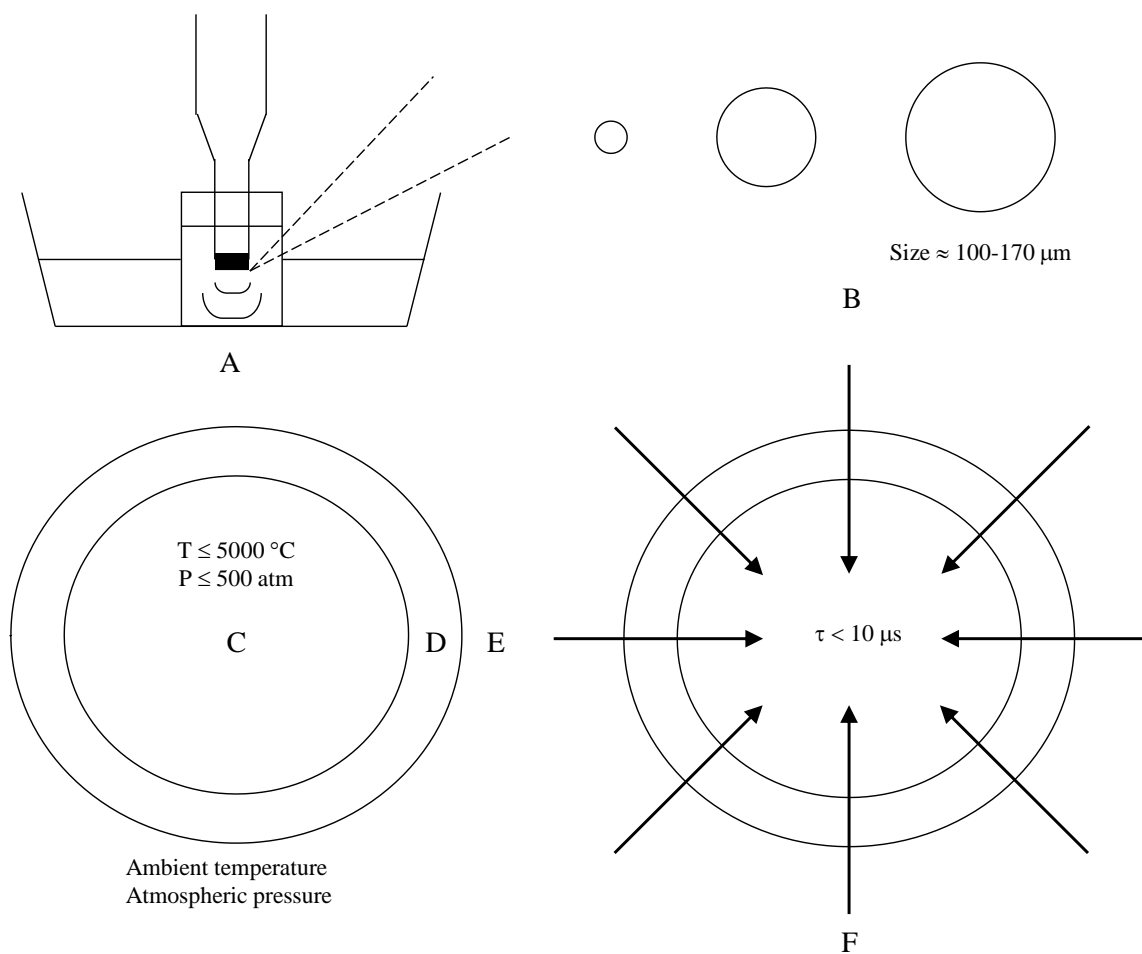
860

861

862

863 **Figure 9.7**

864